Influence of inhibitory circuits in the olfactory bulb on the frequency tuning of mitral cells

Rebecca Miko[1], Christoph Metzner[1] and Volker Steuber[1]
[1] Centre for Computer Science and Informatics Research, University of Hertfordshire, Hatfield, United Kingdom
E-mail: r.miko@herts.ac.uk

Motivation

The olfactory bulb (OB) in mammals is responsible for receiving, processing and relaying olfactory information (odours). Naturalistic odour stimuli have a rich temporal structure, caused by turbulent airflow that mixes the odorant with clean air and other odorants. Recent studies show that this structure contains information about the olfactory scene, for example the distance to an odour source [1,2]. Furthermore, it has been suggested that animals might exploit this structure and extract this information in order to find odour sources [3]. As some of this information may lie in the frequency content of the stimuli [2], we studied input frequency dependent responses of mitral cells (MCs) in the olfactory bulb (OB), the first processing stage in the mammalian olfactory system. Specifically, we investigated whether MCs show frequency tuning and, if they do, how different components of the glomerular layer circuitry shape and determine the tuning.

Method

We used a model of the OB (modified from [4]) containing periglomerular cells (PGCs) and MCs. The cell models have compartments, ion channels and synaptic receptors. The mitral cell model consists of four compartments: soma, apical dendrite, glomerular tuft and lateral dendrite. It also contains the following active ionic currents: fast, spike-generating (INa) and persistent (INaP) sodium currents; a potassium delayed rectifier (IDR); two transient potassium currents (fast-inactivating IA and slow-inactivating IKS); an L-type calcium current (ICaL); and a Ca2+-dependent potassium current (IKCa). The PG cell model consists of three compartments: soma, dendrite and spine. It also contains the following active ionic currents: a fast, spike-generating sodium current (INa); a potassium delayed rectifier (IDR); a transient A-type potassium current (IA); a noninactivating muscarinic potassium current (IM); a low-threshold inactivating (ICaT) and a high-threshold (ICaP/N) calcium current; hyperpolarization-activated current (IH); and a Ca2+-dependent potassium current (IKCa). Finally, synaptic conductances are modelled as double exponentials. We have three different synapses/receptors: pgAMPA (α-amino-3-hydroxy-5-methyl-4-isoxazolepropionic acid), pgNMDA (N-methyl-D-aspartate) and mcGABA (gamma-aminobutyric acid) as shown in Figure 1. Postsynaptic currents were modelled using the equation from [5].

Using these cell models, a model of the MC-PGC motif was created, thus focusing on the recurrent and feed-forward inhibition in the glomerular layer, see Figure 1. The model records the membrane potential at the MC soma.

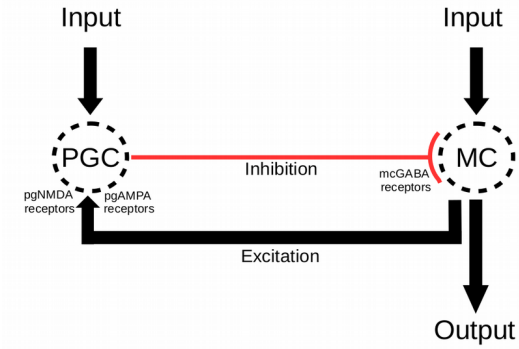

Figure 1: The recurrent and feed-forward inhibition circuitry for the PGC and MC in the OB.

Simple sinusoidal currents of varying frequencies were used as input to the model, using the equation $y(t) = c\sin(2\pi ft + \varphi) + 0.18$. The phase ($\varphi$) was always 0. The strength of the input to the MC (c) was $0.45nA$ for all simulations (run in NEURON), which defined the amplitude of the current, see Figure 2. The PGC input strength was adjusted by multiplying $0.45nA$ by the values: 0.2, 0.3, 0.4, 0.5 and 0.6. The MC-PGC excitation strength varied using W_{exc} values: 2.0, 4.0, 6.0, 8.0 and 10.0. Finally, the PGC-MC inhibition strength varied using W_{inh} values: 1.0, 2.0, 3.0, 4.0 and 5.0. The frequency (f) of the input ranged between $1.0Hz$ and $40.0Hz$ (with a step size of 1.0). The output from the MC was recorded and from this the firing rates were calculated. For each parameter combination (PGC input strength, MC-PGC excitation strength, PGC-MC inhibition strength) we constructed frequency tuning curves by plotting firing rate against input frequency, see Figure 3. From these tuning curves we extracted the peak

resonance frequency and the strength of the tuning Q, which was measured as:

$$Q = \frac{(F_{max} - F_{min})}{<F>} \quad (1)$$

where F_{max} and F_{min} is the maximum and minimum firing rate, and <F> is the mean firing rate over all measured frequencies. Figure 4 summarises the results.

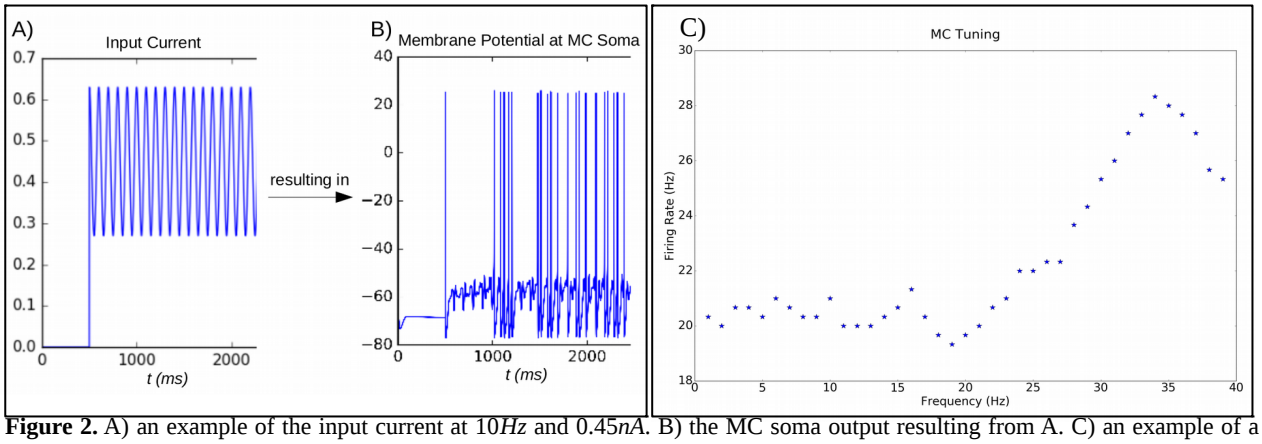

Figure 2. A) an example of the input current at 10*Hz* and 0.45*nA*. B) the MC soma output resulting from A. C) an example of a tuning curve.

Results

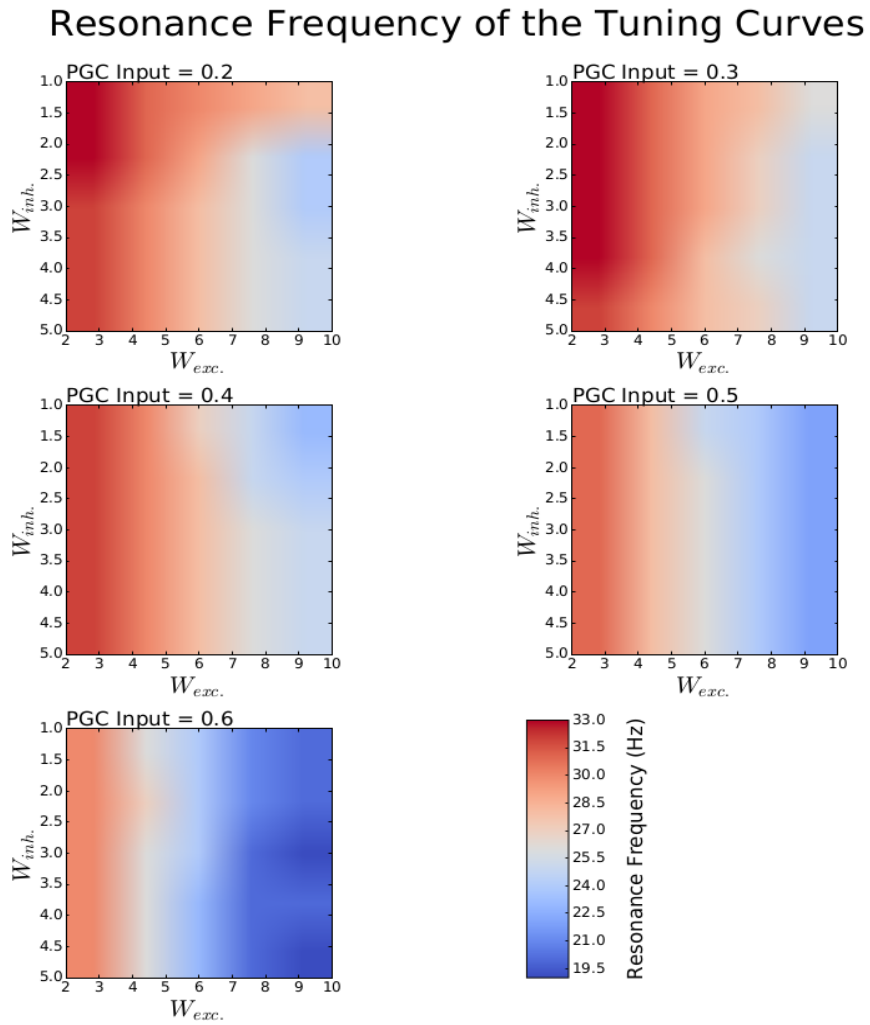

Figure 3: The contour plot shows the distribution of peak resonance frequencies in the tuning curves. The contour bar shows the range in *Hz*, while each individual plot shows the peaks for the different values of PGC input.

We found that the resonance frequency decreased as the excitation of the PGC (both from the input and from the MC) increased, whereas the strength of the PGC inhibition onto the MC did not seem to have a strong effect. Furthermore, the resonance strength increased with the strength of the excitatory connection between the MC and the PGC when the PGC received sufficient external input from olfactory stimuli.

Discussion

These results suggest that the MC can indeed show frequency tuning and that this depends on the strength of the excitatory synaptic input to the PGC, which provide inhibitory input to the MC. However, the observed frequency tuning occurred in a narrow range (19.5*Hz* – 33.0*Hz*). Future work should investigate how the OB could use this frequency tuning to obtain information about the surrounding olfactory scene.

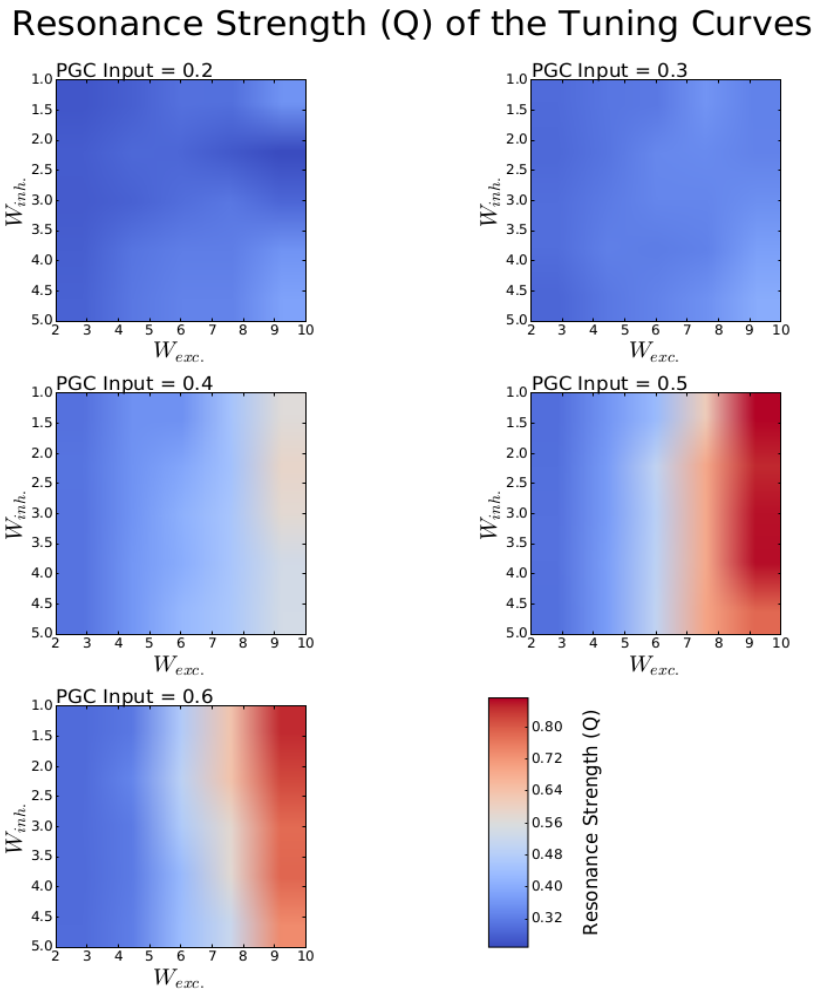

Figure 4: The contour plot shows the resonance strength Q, as defined in Eq. 1.

Acknowledgments

We thank Dr Michael Schmuker for comments on the abstract.

References

[1] Celani, A., Villermaux, E. and Vergassola, M.: **Odor landscapes in turbulent environments.** Physical Review X, 4(4), p.041015, 2014.

[2] Schmuker, M., Bahr, V. and Huerta, R.: **Exploiting plume structure to decode gas source distance using metal-oxide gas sensors.** Sensors and Actuators B: Chemical, 235, pp.636-646, 2016.

[3] Jacob, V., Monsempès, C., Rospars, J.P., Masson, J.B. and Lucas, P.: **Olfactory coding in the turbulent realm.** PLoS Computational Biology, 13(12), p.e1005870, 2017.

[4] Li, G. and Cleland, T.A.: **A two-layer biophysical model of cholinergic neuromodulation in olfactory bulb.** Journal of Neuroscience, 33(7), pp.3037-3058, 2013.

[5] Brea, J.N., Kay, L.M. and Kopell, N.J.: **Biophysical model for gamma rhythms in the olfactory bulb via subthreshold oscillations.** Proceedings of the National Academy of Sciences, 106(51), pp.21954-21959, 2009.